in stable molecules is well justified, and with the results of theory should lead to a better understanding of the geometrical changes in chemical reactions. Further accurate studies on a number of related molecules are currently in progress,

References and Notes

(1) R. Hoffmann and R. B. Woodward, *Science*, **167**, 825–831 (1970).
(2) For example, D. Ginsburg, *Acc. Chem. Res.*, **5**, 249–256 (1972); J. Haywood-Farmer, *Chem. Rev.*, **74**, 315–350 (1974).
(3) M. J. S. Dewar and W. W. Schoeller, *J. Am. Chem. Soc.*, **93**, 1481–1482 (1971).
(4) (a) R. Hoffmann and W. D. Stohrer, *J. Am. Chem. Soc.*, **93**, 6941–6948 (1971); (b) M. J. S. Dewar and D. H. Lo, *ibid.*, **93**, 7201–7207 (1971).
(5) A. K. Cheng, F. A. L. Anet, J. Mioduski, and J. Meinwald, *J. Am. Chem. Soc.*, **98**, 2887–2891 (1974).
(6) L. A. Paquette and W. E. Volz, *J. Am. Chem. Soc.*, **98**, 2910–2917 (1976).
(7) L. A. Paquette, W. E. Volz, M. A. Beno, and G. G. Christoph, *J. Am. Chem. Soc.*, **97**, 2562–2563 (1975).
(8) U. W. Arndt and B. T. M. Willis, "Single Crystal Diffractometry", Cambridge University Press, New York, N.Y., 1966, p 287.
(9) W. R. Busing and H. A. Levy, *J. Chem. Phys.*, **26**, 563–568 (1957).
(10) $R_1 = \sum ||F_i| - |F_{av}||/\sum|F_{av}|$, $R_2 = \{\sum_i[(F_i^2 - F_{av}^2)^2/\sigma^2(F_i^2 - F_{av}^2)]/\sum[F_{av}^4/\sigma^2(F_i^2 - F_{av}^2)]\}^{1/2}$.
(11) E. R. Howells, D. C. Phillips, and D. Rogers, *Acta Crystallogr.*, **3**, 210–214 (1950).
(12) G. Germain, P. Main, and M. M. Woolfson *Acta Crystallogr., Sect. B*, **26**, 274–285 (1970).
(13) A. C. Larson, *Acta Crystallogr.*, **23**, 664–665 (1967).
(14) The function minimized in the least-squares refinement was $\sum\{F_o^2 - F_c^2)^2/\sigma^2(F_o^2)\}$, $R = \sum||F_o| - |F_c||/\sum|F_o|$, $R_w = \{\sum w(F_o^2 - F_c^2)^2/\sum_w F_o^4\}^{1/2}$ where $w = 1/\sigma^2(F_o^2)$. The "goodness of fit" is defined as $\{\sum w(F_o^2 - F_c^2)^2/(n_o - n_p)\}^{1/2}$. Atomic form factors for C and N were taken from the International Tables,[15] and that for hydrogen from Stewart, Davidson, and Simpson.[16]
(15) "International Tables for X-Ray Crystallography", Vol. III, Kynoch Press, Birmingham, England, 1962, pp 202–203.
(16) R. F. Stewart, E. R. Davidson, and W. T. Simpson, *J. Chem. Phys.*, **42**, 3175–3187 (1965).
(17) S. C. Abrahams and E. T. Keve, *Acta Crystallogr., Sect. A*, **27**, 157–165 (1971).
(18) See paragraph at end of paper regarding supplementary material, which consists of (I) observed and calculated structure factor amplitudes; (II) thermal motion librational model parameters; (III) results of least-squares

planes calculations; and (IV) interatomic contacts of less than 3.5 Å.
(19) V. Schomaker and K. N. Trueblood, *Acta Crystallogr., Sect. B*, **24**, 63–76 (1968).
(20) R. F. Picone, M. T. Rogers, and M. Newman, *J. Chem. Phys.*, **61**, 4808–4813 (1974).
(21) A. D. Walsh, *Trans. Faraday Soc.*, **45**, 179–190 (1949).
(22) W. A. Bernett, *J. Chem. Educ.*, **44**, 17–24 (1967); R. Hoffmann, *Tetrahedron Lett.*, 2907–2909 (1970).
(23) For example, M. Charton in "The Chemistry of Alkenes", Vol. II, J. Zabricky, Ed., Wiley-Interscience, New York, N.Y., 1970, Chapter 10, pp 511–610.
(24) (a) R. E. Long, H. Maddox, and K. N. Trueblood, *Acta Crystallogr., Sect. B*, **25**, 2083–2094 (1969); (b) A. Hartman and F. L. Hirschfield, *ibid.*, **20**, 80–82 (1966); (c) C. J. Fritchie, *ibid.*, **20**, 27–36 (1966).
(25) O. Bastiansen, F. N. Fritsch, and K. Hedberg, *Acta Crystallogr.*, **17**, 538–543 (1964).
(26) Y. C. Wang and S. H. Bauer, *J. Am. Chem. Soc.*, **94**, 5651–5657 (1972).
(27) The complexity and low symmetry of the molecule did not permit optimization of all the independent geometry parameters simultaneously in their study; indeed, constraints on two or more parameters were required for convergence of their least-squares procedure to be achieved at all. Ten models, differing in which 2 of 14 parameters were constrained, each were found to give satisfactory agreement with the observed radial distribution function. The constraints consisted chiefly of the imposition of equality on the bond distances C(1)–C(5), C(1)–C(2), and C(4)–C(5) or C(2)–C(3). We are consequently inclined to view the results as approximate. No estimates of the errors in the derived structure were given. However, a measure of the reliability of their results is suggested by the range of values of the bonding parameters for the ten models: C_1–C_5, 0.030 Å; C_1–C_2, 0.030 Å; C_4–C_5, 0.031 Å; C_2–C_3, 0.046 Å; and C_2–C_8, 0.032 Å. These ranges recommend esd's of *at least* 0.015 Å for the distances in Figure 5.
(28) M. I. Davis and T. W. Muecke, *J. Phys. Chem.*, **74**, 1104–1108 (1970).
(29) M. Traetteberg, *J. Am. Chem. Soc.*, **86**, 4265–4270 (1964).
(30) R. E. Davis and A. Tulinsky, *J. Am. Chem. Soc.*, **88**, 4583–4588 (1966).
(31) M. Dobler and J. D. Dunitz, *Helv. Chim. Acta*, **48**, 1429–1440 (1965).
(32) C. J. Brown, *J. Chem. Soc.*, 3278–3285 (1953).
(33) (a) D. J. Cram and J. M. Cram, *Acc. Chem. Res.*, **4**, 204–213 (1971); (b) Y. Kai, N. Yasuoka, and N. Kasai, *Acta Crystallogr., Sect. B*, **33**, 754–762 (1977).
(34) L. A. Paquette, T. G. Wallis, T. Kempe, G. G. Christoph, J. P. Springer, and J. Clardy, *J. Am. Chem. Soc.*, **99**, 6946–6954 (1977).
(35) The double bonds C(3)–C(4) and C(6)–C(7) are well localized and essentially planar; the geometry recommends fully occupied p–π lobes perpendicular to the C(2)–C(3)–C(4)–C(5) and C(5)–C(6)–C(7)–C(8) planes. For [2.2]-metacyclophane the orientations of the p orbitals are probably accurate, but the hybridization and orbital population are certainly somewhat altered (see ref 33) due to the alterations from normal benzene geometry. The assumptions (2) and (3) are thus likely to be less accurate for [2.2]meta-cyclophane than for 1-cyanosemibullvalene.
(36) R. S. Mulliken, C. A. Rieke, D. Orloff, and H. Orloff, *J. Chem. Phys.*, **17**, 1248–1267 (1949).
(37) R. Askani, R. Gleiter, E. Heilbronner, V. Hornung, and H. Musso, *Tetrahedron Lett.*, 4461–4466 (1971).
(38) E. Heilbronner and A. Schmelzer, *Helv. Chim. Acta*, **58**, 936–967 (1975).
(39) R. C. Bingham, M. J. S. Dewar, and D. H. Lo, *J. Am. Chem. Soc.*, **97**, 1294–1301 (1975).
(40) T. A. Halgren and W. N. Lipscomb, *J. Chem. Phys.*, **58**, 1569–1591 (1973).

Mechanism of Formation of Grignard Reagents

E. A. Vogler,* R. L. Stein, and J. M. Hayes[1]

Department of Chemistry, Indiana University, Bloomington, Indiana 47401. Received November 11, 1977

Abstract. Experiment shows that there is no carbon kinetic isotope effect in the formation of CH_3MgI from CH_3I ($k_{12}/k_{13} = 0.9992$, $\sigma = 0.0005$). Calculations indicate that an observable isotope effect should accompany this reaction if it proceeds by an inner-sphere electron-transfer mechanism in which breakage of the carbon–halogen bond must be involved in the rate-determining step. Accordingly, it is proposed that the alternative mechanism must be followed, with the rate-determining step involving formation of a radical–ion pair by outer-sphere electron transfer from the magnesium to the organic halide.

The formation of the Grignard reagent from alkyl halide and magnesium is of continued mechanistic interest.[2-8] It is generally concluded from stereochemical, kinetic, and CIDNP studies that alkyl radicals are intermediates. However, the route by which radicals are formed and the relevance of such

an intermediate to the formation of the Grignard reagent remains largely undefined.
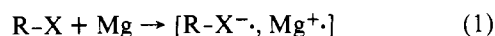
Two alternative rate-determining steps can be envisioned. One involves electron transfer from the magnesium surface (here represented in monomeric form for simplicity) to the

**Table I.** Kinetic Isotope Effect for Grignard Reagent Formation at 34.5 °C[a]

$\delta^{13}C_{PDB}CH_3I$, ‰	$\delta^{13}C_{PDB}CH_4$, ‰	Yield, %	k_{12}/k_{13}
-79.04 ± 0.15	-79.01 ± 0.17	32.7	1.0000
-79.26 ± 0.09	-77.23 ± 0.21	42.7	0.9971
-79.33 ± 0.32	-78.42 ± 0.14	38.5	0.9987
-81.23 ± 0.21	-81.63 ± 0.09	36.6	1.0006
-80.81 ± 0.09	-78.89 ± 0.09	6.7	0.9978
-80.84 ± 0.45	-81.14 ± 0.10	39.4	1.0004
-80.84 ± 0.45	-80.54 ± 0.11	25.9	0.9996
		Av k_{12}/k_{13} = 0.9992 $\pm$ 0.0005	

[a] Indicated uncertainties are standard deviations. All isotopic analyses were performed in triplicate.

alkyl halide, forming a tight radical–ion pair.

$$R-X + Mg \rightarrow [R-X^{-}\cdot, Mg^{+}\cdot] \qquad (1)$$

The alternative involves transfer of the halogen atom to magnesium, forming a loose radical pair. In this case, the carbon–halogen bond is broken in the rate-determining step.

$$R-X + Mg \rightarrow R\cdot + \cdot MgX \qquad (2)$$
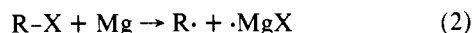
Subsequently, the products of either of these rate-determining steps can directly form product, RMgX, although the tight radical–ion pair might first collapse to the loose radical pair.

Both alternative rate-determining steps are electron-transfer reactions and, as such, can be conveniently viewed in terms of oxidation–reduction mechanisms. According to the classification of such reactions,[9] routes 1 and 2 correspond to outer-sphere and inner-sphere electron-transfer processes respectively. In the former, the electron given up by the reducing agent (Mg) is transferred to the oxidizing agent (RX) with no net bond breakage or formation in either reaction partner. The latter mechanism, however, involves transfer of the halogen atom from the organohalide to magnesium, a process involving both bond breakage and formation. Given this contrast, it follows that a study of kinetic isotope effects can allow a choice between the inner-sphere and outer-sphere electron-transfer mechanisms. A primary carbon isotope effect is expected in route 2, none is expected in route 1.

The sensitivity of the mechanistic test depends upon the magnitude of the isotope effect which would be expected to accompany route 2. Although this cannot be known directly, the isotope effect prevailing in a simple carbon–halogen bond homolysis reaction, e.g.,

$$CH_3X \rightarrow CH_3\cdot + X\cdot \qquad (3)$$
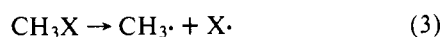
can be used to estimate it. Carbon kinetic isotope effects have not been measured for alkyl–halide homolysis reactions, but the isotope effect for the hypothetical equilibrium,

$$CH_3X \rightleftharpoons CH_3\cdot + X\cdot \qquad (4)$$
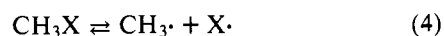
can be calculated[10,11] and used as a measure of the maximum value of the kinetic isotope effect for bond homolysis.

In this report, we present, first, experimental measurements of the carbon kinetic isotope effect in the reaction of methyl iodide with magnesium in diethyl ether and, second, a calculation of the equilibrium isotope effect for the homolysis of methyl iodide. Taken together, the results of these studies suggest that outer-sphere electron transfer rather than inner-sphere electron transfer is the rate-determining step in the formation of the alkyl Grignard reagent.

Results

Measurement of the Isotope Effect. Experimental measurements of the isotopic fractionation accompanying the formation of methyl magnesium iodide are summarized in Table I, in which the carbon isotopic composition of methane derived from hydrolysis of the methyl magnesium iodide is compared with that of the methyl iodide from which the Grignard reagent was formed.

$$CH_3I \xrightarrow[Et_2O]{Mg} CH_3MgI \qquad (5)$$

$$CH_3MgI \xrightarrow{H_2O} CH_4 + MgI(OH) \qquad (6)$$
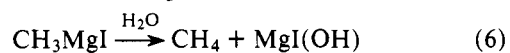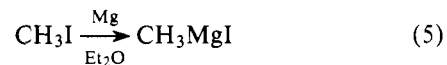
The isotopic compositions are reported in terms of $\delta^{13}C_{PDB}$, where $\delta^{13}C_{PDB} = [(R_{sample}/R_{PDB}) - 1]10^3$, $R = {}^{13}C/{}^{12}C$, and PDB indicates the PeeDee Belemnite isotropic standard R_{PDB} = 0.0112372. The units for δ are denoted by the symbol ‰, and are termed "per mil".[12] The tabulated isotope effects were calculated from the data using

$$\left(\frac{k_{13}}{k_{12}} - 1\right) \log\left[(1-f)\frac{101124 + 1.124\delta_0}{101124 + 1.124\delta_p}\right]$$
$$= \log\left[\left(1 + \frac{\delta_0 - \delta_p}{\delta_0 + 10^3}\right)\left(\frac{f}{1-f}\right)\right] \qquad (7)$$

where f is the fractional degree of completion ($0 \le f \le 1.0$), and δ_0 and δ_p represent the $\delta^{13}C_{PDB}$ values for the starting reactant (CH$_3$I) and pooled product (CH$_4$ from CH$_3$MgI hydrolysis), respectively. Equation 7 has been recast in terms of δ, from an expression derived by Bigeleisen and Wolfsburg,[13] and is exact for all values of δ and for ($0 < f < 1$).

The results given in Table I show that the formation of the Grignard reagent in this system proceeds with no observable kinetic isotope effect. As noted, this experimental result constitutes only one half of a necessary comparison. While the absence of an isotope effect strongly favors route 1, it must also be shown that the isotope effect which would accompany the inner-sphere electron-transfer mechanism, if it occurred, is large enough to be detectable. In the absence of experimental determinations of carbon kinetic isotope effects prevailing in carbon–halogen bond homolyses, it is necessary to calculate the theoretical equilibrium isotope effect[10,11] and to base the comparison upon that result.

Calculation of the Equilibrium Isotope Effect. Equilibrium isotope effects were calculated using a program developed by Burton, Sims, Wilson, and Fry.[14] The calculations incorporate the hypothetical equilibrium represented by eq 4, in which methyl radical is taken as a model for the intermediate in route 2, this radical being assumed to resemble closely the intermediate that would directly follow rate-limiting inner-sphere electron transfer. The equilibrium carbon isotope effect is the carbon isotope ratio of the reactant R_{CH_3X}, divided by the carbon isotope ratio of the products, $R_{CH_3\cdot}$. It can also be expressed in terms of the ratio of complete partition functions, Q, for the species involved in the equilibrium.

$$\frac{K_{12}}{K_{13}} = \frac{[{}^{12}CH_3\cdot][{}^{13}CH_3X]}{[{}^{13}CH_3\cdot][{}^{12}CH_3X]}$$

$$= \frac{R_{CH_3X}}{R_{CH_3\cdot}} = \frac{(Q_{{}^{12}CH_3\cdot})(Q_{{}^{13}CH_3X})}{(Q_{{}^{13}CH_3\cdot})(Q_{{}^{12}CH_3X})} \qquad (8)$$

Calculation of the equilibrium isotope effect requires knowledge of molecular geometries, nuclidic masses, and force constants for all bonds. In the case of methyl halides, all of the required parameters are well known[15,16] and are listed in Table II. The methyl radical is assumed to possess D_{3h} geometry[17,18] with the force constants for a C–H stretch, a hydrogen out-of-plane bending, and a H–C–H bending mode being required in the calculation. The C–H stretching valence force constant

Table II. Force Constants Used in the Calculation of Equilibrium Isotope Effects

| Compd | Stretching,[a,b] mdyn · Å⁻¹ | | Bending,[a] mdyn · Å · rad⁻² | | |
	C–X	C–H	H–C–H	H–C–X	Out of plane
CH_3I	2.309 (2.139)	5.006 (1.095)	0.450	0.444	
CH_3Cl	3.386 (1.78)	4.969 (1.095)	0.468	0.566	
CH_3·		5.15[c] (1.079)[d]	0.40[c]		0.070[c]
			0.75		

[a] See ref 11 unless otherwise indicated. [b] Bond length in angstroms in parentheses; see ref 17. [c] See text. [d] See ref 18.

Table III. Theoretical Equilibrium Isotope Effects[a,b]

| H–C–H bending[b] force constant, mdyn · Å · rad⁻² | Compd | | | |
| | CH_3I | | CH_3Cl | |
	K_H/K_D	K_{12}/K_{13}	K_H/K_D	K_{12}/K_{13}
0.40	1.246	1.029		
0.60	1.103	1.027	1.169	1.035
0.75	1.019	1.019		

[a] Isotope effect values calculated for 25 °C. [b] See text.

for the methyl radical has been obtained by the method of estimation derived by Gordy.[19] In this procedure, the bond length[20] of the C–H bond in ethylene has been used as a model for the calculation of the C–H stretch of methyl radical. The hydrogen out-of-plane bending mode force constant has been obtained by iterative fitting of the vibrational mode at 607 cm⁻¹. The value of the H–C–H bending mode force constant is unknown and cannot be closely estimated. Therefore, the value of this constant has been varied between extremes in order to allow calculation of maximum and minimum equilibrium isotope effects. The resulting values of the methyl radical force constants are summarized in Table II.

Calculated values for both the hydrogen and carbon equilibrium isotope effects are given in Table III. Three different values of the H–C–H bending mode force constant have been considered, and the observed effects of this variation allow the probable value of the carbon isotope effect to be determined quite specifically. On the one hand, when methyl iodide is considered as the reactant and a minimal value for the H–C–H bending mode force constant is used, the calculated carbon isotope effect is 2.9%. Because the associated hydrogen isotope effect is already improbably large[21] (25%) and because further decreases in the force constant lead to still more extreme values, we conclude that the equilibrium carbon isotope effect is unlikely to exceed 3%. On the other hand, if a large value is assigned to the force constant (the value chosen is, in fact, 11% greater than the H–C–H bending force constant in ethylene), the calculated carbon isotope effect is still nearly 2%, while the hydrogen isotope effect has become improbably small (1.9%).[21,22] It is, therefore, concluded that the equilibrium isotope effect for reaction 4 lies between 2 and 3%.

Discussion

The observed *kinetic* isotope effect can be usefully compared to a calculated *equilibrium* isotope effect even though the latter is purely thermodynamic in origin. The kinetic isotope effect can be expressed as the product of an imaginary frequency factor and a zero-point energy term, as noted in eq 9.[23]

$$k_{12}/k_{13} = (\nu_{12L}/\nu_{13L})[ZPE] \qquad (9)$$

For dissociative reactions in which the imaginary frequency term is unity (those cases in which there is no motion of the isotopically substituted atom along the reaction coordinate), the equilibrium isotope effect sets an upper limit for the kinetic isotope effect. This occurs because the equilibrium isotope effect represents the maximum value of the zero-point energy

term, this maximum being approached when the product of the equilibrium strongly resembles the rate-determining transition state. For the reaction being modeled here, however, and for all reactions in which there is motion of the isotopically substituted atom along the reaction coordinate, the imaginary frequency term will be >1. In these cases, the maximum kinetic isotope effect will exceed the equilibrium isotope effect and, particularly for reactions having late transition states, observed kinetic isotope effects can exceed calculated equilibrium isotope effects. It happens, therefore, that, for reactions of this type, the equilibrium isotope effect can be taken as a useful estimate of the kinetic isotope effect, being an underestimate if contributions from reaction coordinate motion are significant and the transition state is very late, and being an overestimate if these circumstances are reversed.

Because the similarity in substituent effects lends support to the parameters chosen to describe the methyl radical, it is interesting to compare the calculated equilibrium isotope effects with experimentally determined kinetic isotope effects for *heterolytic* cleavage of a carbon–halogen bond. When an intermediate value is assigned to the H–C–H bending mode force constant, the calculated hydrogen isotope effects are 10.3% for methyl iodide and 16.9% for methyl chloride (Table III). This predicted substituent effect is in good agreement with experimental observations, which show that the α-hydrogen isotope effect for heterolysis of an alkyl iodide via an S_N1 mechanism is 9%, while that for an alkyl chloride is 16%.[24]

It is well to ask, quite apart from the adequacy of the calculations, whether the methyl radical is a good model of the intermediate formed by inner-sphere electron transfer in route 2. If the strength of interaction between the alkyl radical and the magneseous halide radical (·MgX) were comparable with the strength of the carbon–iodide bond in methyl iodide, the methyl radical would be a poor model. However, it has been shown that the reaction of optically active 1-iodo-1-methyl-2,2-diphenylcyclopropane with magnesium in THF proceeds with greater than 98% racemization.[6] Therefore, the strength of interaction between the alkyl radical and the magneseous iodide radical must be weak, inasmuch as retention of configuration would have been expected if the interaction had been strong. Further, during the formation of a Grignard reagent, it is often observed that the alkyl radicals can undergo side reactions such as combination, disproportionation, and reaction with solvent.[2,6] These observations suggest that the alkyl radical must have considerable mobility on the surface of the magnesium, and that the methyl radical represents an appropriate model.

Conclusions

The formation of methyl magnesium iodide proceeds with no carbon kinetic isotope effect, although the calculated equilibrium isotope effect lies between two and three percent if the reaction proceeds via route 2. Because the detection limits of the procedure are on the order of 0.1%, a kinetic isotope effect should have been observed even if rate-determining inner-sphere electron transfer did occur and happened to involve a transition state that did not closely resemble methyl
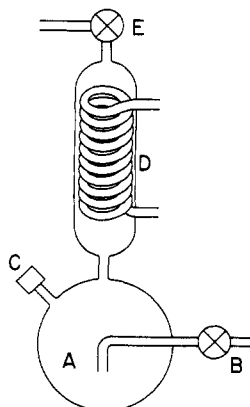
Figure 1. Reaction vessel for the production of Grignard reagent: A, 25-mL round-bottom flask; B, side arm valve; C, injection port; D, reflux condenser; E, vacuum valve.

radical. The alternative must, therefore, be chosen, and we conclude that route 1, in which outer-sphere electron transfer forms the rate-determining step, more closely represents the mechanism of this reaction. This conclusion is in agreement with that of Walborsky,[6] and is consistent with the results of electrochemical reductions of alkyl halides.[25]

Experimental Section

Apparatus. The Grignard reaction was carried out in an apparatus (Figure 1) consisting of a 25-mL round-bottom flask (A) to which had been sealed a side arm valve (B) which served as an inlet for N_2 purge gas, a septum port (C) for the introduction of solvents and reactants, and a reflux condenser (10 cm in height, 1 cm in diameter).

The mercury diffusion pumped vacuum apparatus (Figure 2) used for the recovery of the CH_4 resulting from the hydrolysis of the Grignard reagent consisted of a positive displacement mercury piston (F) fitted with a two-way vacuum valve (G) which allowed the raising and lowering of the mercury. The total sweep volume of the piston was ~1 L. Valves H and I served as the sample introduction or withdrawal ports. The liquid-nitrogen-cooled high efficiency trap (K) and the high capacity trap (L) were removable and in place during the CH_4 introduction step.

Production and Hydrolysis of the Methyl Grignard Reagent. Approximately 20 mg of Mg turnings and 10 mL of anhydrous diethyl ether were added to the dry 25-mL round-bottom flask through the septum port while purging with N_2 (A, Figure 1). The mixture was stirred vigorously with a magnetic stirring bar and the ether was brought to reflux temperature. A known quantity (~0.5 mmol) of dry CH_3I was injected into the refluxing ether.

After reaction (a variable time of reaction was used, 5–30 min), the cooling water supply to the reflux condenser was shut off and, under a fast flow of N_2, the diethyl ether was evaporated. Subsequently, the reaction flask was attached to trap L (Figure 2) and evacuated through valve E (Figure 1) to assure that most of the diethyl ether was removed.

Approximately 5 mL of H_2O was injected into the reaction flask through the septum port to hydrolyze the Grignard reagent. The resulting CH_4 was led into the piston through traps L and K (Figure 2) by allowing the gas to expand into the volume created in the piston by lowering the mercury level. Traps L and K were held at −198 °C (liquid nitrogen) to assure that only CH_4 would pass into the piston. The volume of the system was large enough to assure that all of the CH_4 must be in the gaseous state to support the vapor pressure of methane at liquid-nitrogen temperatures. Complete mixing of the gas was assured by raising and lowering the mercury level in the piston. Aliquots of the gas were taken for combustion by expanding the CH_4 from the piston into an evacuated flask.

Combustion and Determination of the Isotopic Compositions of CH_3I and CH_4. Both CH_3I and CH_4 samples were combusted in an oven at 1200 °C in the presence of an excess of oxygen and a Pt ribbon catalyst. The CO_2 resulting from the combustion was separated from water by sublimation at −117 °C (ethanol slush). The purified CO_2
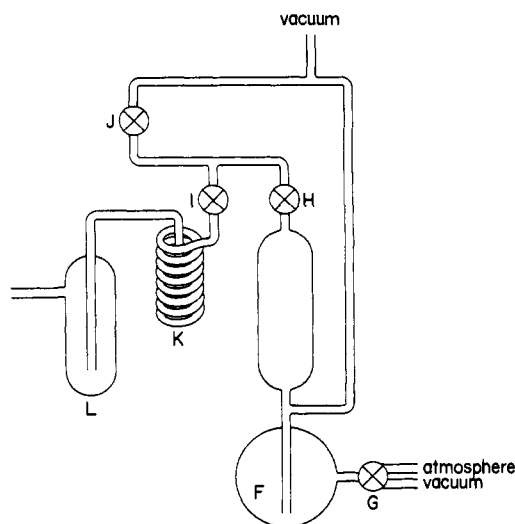

Figure 2. Apparatus for collection of methane (regulation of the pressure in flask F controls the level of mercury in the cylindrical volume above the flask, forming a 1-L positive displacement piston allowing quantitative gas transfer): G, H, I, J, vacuum valves; K, L, liquid-nitrogen-cooled traps.

was transferred in a breakseal tube[26] to the inlet system of an isotope ratio mass spectrometer like that described by McKinney et al.[27]

References and Notes

(1) Also Department of Geology.
(2) M. S. Karasch and O. Reinmuth, "Grignard Reactions of Non-Metallic Substances", Prentice Hall, New York, N.Y., 1954.
(3) E. C. Ashby, *Quart. Rev.*, **21**, 259–285 (1967).
(4) H. M. Walborsky and A. E. Young, *J. Am. Chem. Soc.*, **83**, 2595–2596 (1961).
(5) M. P. Khyrak, *Reakts. Sposobn. Org. Soedin.*, **1**, 120–127 (1964), cited in *Chem. Abstr.*, **61**, 13165a (1964).
(6) H. M. Walborsky and M. S. Aronoff, *J. Organomet. Chem.*, **51**, 31–53 (1973).
(7) H. W. H. J. Bodewitz, C. Blomberg, and F. Bickelhaupt, *Tetrahedron*, **29**, 719–725 (1973).
(8) R. J. Rogers, J. L. Mitchell, Y. Fujiwara, and G. M. Whitesides, *J. Org. Chem.*, **39**, 857–858 (1974).
(9) H. Taube, *J. Chem. Educ.*, **45**, 452–460 (1968).
(10) M. Wolfsberg, *Ann. Rev. Phys. Chem.*, **20**, 449–478 (1969).
(11) S. R. Hartshorn and V. J. Shiner, *J. Am. Chem. Soc.*, **94**, 9002–9012 (1972).
(12) H. Craig, *Geochim. Cosmochim. Acta*, **12**, 133–149 (1957).
(13) J. Bigeleisen and M. Wolfsberg, *Adv. Chem. Phys.*, **1**, 15–76 (1952).
(14) G. W. Burton, L. B. Sims, J. C. Wilson, and A. Fry, *J. Am. Chem. Soc.*, **99**, 3371–3373 (1977).
(15) W. T. King, I. M. Mills, and B. L. Crawford, *J. Chem. Phys.*, **27**, 455–457 (1957).
(16) J. Aldous and I. M. Mills, *Spectrochim. Acta*, **19**, 1567–1584 (1963).
(17) G. Hertzburg, *Proc. R. Soc. London, Ser. A*, **262**, 291–317 (1961).
(18) L. Y. Tan and A. M. Winer, *J. Chem. Phys.*, **57**, 4028–4037 (1977).
(19) W. Gordy, *J. Chem. Phys.*, **14**, 305–320 (1946).
(20) B. N. Cyvin and S. J. Cyvin, *Acta Chem. Scand.*, **17**, 1831–1842 (1968).
(21) J. A. Hirsch, "Concepts in Theoretical Organic Chemistry", Allyn and Bacon, Boston, Mass., 1974, pp 155–157.
(22) J. Y. Kirsch in "Isotope Effects on Enzyme-Catalyzed Reactions", W. W. Cleland, M. H. O'Leary, and D. B. Northrop, Ed., University Park Press, Baltimore, Md., 1977, pp 100–121.
(23) M. H. O'Leary in ref 22, pp 233–251.
(24) V. J. Shiner, *ACS Symp. Ser.*, **No. 11**, 163–183 (1975) (see p 177).
(25) J. L. Webb, C. K. Mann, and H. M. Walborsky, *J. Am. Chem. Soc.*, **92**, 2042–2051 (1970).
(26) D. J. DesMarais and J. M. Hayes, *Anal. Chem.*, **48**, 1651 (1976).
(27) C. R. McKinney, J. M. McCrea, S. Epstein, H. A. Allen, and H. C. Urey, *Rev. Sci. Instrum.*, **21**, 724–730 (1950).